BIOCHEMISTRY
including biophysical chemistry & molecular biology

Article

pubs.acs.org/biochemistry

Divergent Kinetics Differentiate the Mechanism of Action of Two HDAC Inhibitors

Astrid M. Kral,*[,¶] Nicole Ozerova,[†] Joshua Close, Joon Jung,[‡] Melissa Chenard, Judith Fleming,[#] Brian B. Haines, Paul Harrington,[§] John Maclean, Thomas A. Miller, Paul Secrist,[∥] Hongmei Wang, and Richard W. Heidebrecht, Jr.[⊥]

Merck & Co., Inc., 33 Avenue Louis Pasteur, Boston, Massachusetts 02115, United States

Supporting Information

ABSTRACT: Histone deacetylases (HDACs) play diverse roles in many diseases including cancer, sarcopenia, and Alzheimer's. Different isoforms of HDACs appear to play disparate roles in the cell and are associated with specific diseases; as such, a substantial effort has been made to develop isoform-selective HDAC inhibitors. Our group focused on developing HDAC1/HDAC2-specific inhibitors as a cancer therapeutic. In the course of characterizing the mechanism of inhibition of a novel HDAC1/2-selective inhibitor, it was determined that it did not exhibit classical Michaelis−Menten kinetic behavior; this result is in contrast to the seminal HDAC inhibitor SAHA. Enzymatic assays, along with a newly developed binding assay, were used to determine the rates of binding and the affinities of both the HDAC1/2-selective inhibitor and SAHA. The mechanism of action studies identified a potential conformational change required for optimal binding by the selective inhibitor. A model of this putative conformational change is proposed.

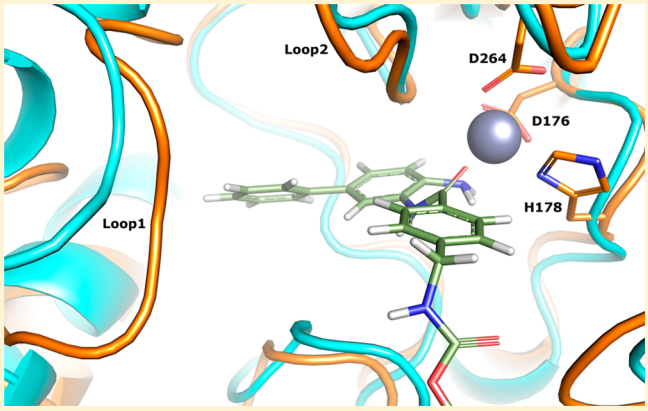

Epigenetic changes, such as DNA methylation or histone acetylation, can alter gene expression in the absence of direct DNA sequence mutations. The acetylation status of histones and other proteins is regulated by the opposing actions of histone acetyltransferases (HATs) and histone deacetylases (HDACs), and some of these changes have been implicated in the development of cancer. Dynamic histone acetylation is involved in the regulation of many genes including some that are critical for differentiation, proliferation, and apoptosis. Some nonhistone proteins that have been shown to undergo acetylation are involved in DNA repair, apoptosis, mitosis, and cell signaling.[1]

HDACs are divided into four different classes. Classes 1, 2, and 4 ("classical HDACs") are Zn^{2+}-dependent and share a similar catalytic mechanism. Class 3 HDACs, also known as Sirtuins, are NAD^{+}-dependent (reviewed in ref 1). The Class 1 proteins (HDACs 1, 2, 3, and 8) are ubiquitously expressed, whereas Classes 2 and 4 are expressed in a tissue-specific manner. Most of the classical HDACs are found in large protein complexes that, among other things, can target the HDACs to a specific site on the chromosome. Some of these proteins are transcription factors involved in growth, apoptosis, and differentiation such as the estrogen receptor and HIF1α.[1] Other proteins in the complex are capable of regulating the deacetylase activity itself. Due to the similarity of mechanism shared by the classical HDACs, HDAC inhibitors can hit multiple members of this group.[1]

Mutations and aberrant expression of these protein-modifying enzymes have been noted in many cancers. Evidence for the critical role of HDACs 1 and 2 in the development of several types of cancer is published on an ever-increasing basis. Some of these data connect HDAC1/2-containing repressor complexes to silencing or downregulating tumor suppressor genes such as pRB, p53, and p21.[2] As a consequence, HDACs 1 and 2 can function to promote proliferation and inhibit apoptosis. HDAC1 has an additional role in inducing resistance to chemotherapy.[1]

There is much evidence for the important role of HDAC1 on cell proliferation. HDAC1 knockout in mice results in an upregulation of $p21^{WAF1}$ and $p27^{KIP1}$, leading to cell cycle arrest and consequent embryonic lethality.[1] RNAi-induced knockdown of HDAC1 expression in human tumor cell lines results in an inhibition of proliferation and induction of apoptosis.[3] Clinically, HDAC1 overexpression has been observed in approximately 60% of patients with gastric cancer.[4]

HDAC2 appears to have a critical role in APC mutant colon tumorigenesis [5] and may play an important role in the rate of progression of colon tumor development.[6] HDAC2 down-regulation in ER-positive breast cancer results in reduced levels of ER, thus improving tamoxifen efficacy.[7]

Received: July 15, 2013
Revised: December 14, 2013
Published: January 22, 2014

While small-molecule HDAC inhibitors such as SAHA are showing clinical efficacy in the treatment of particular cancer types, these drugs have associated toxicities that may impact their widespread use as cancer therapies.[8] Current HDAC inhibitors in the clinic can be classified as "pan-HDAC" inhibitors as they inhibit the function of multiple HDACs. This lack of selectivity may negatively influence the tolerability and, therefore, the ultimate efficacy of these drugs. Efficacy may also be impacted by the achievable exposures of the currently available HDAC inhibitors.

In order to improve the therapeutic index of pan-HDAC inhibitors, we sought to identify HDAC1/2-selective inhibitors based on the concept that more selective inhibitors would reduce toxicities and increase clinical efficacy.[8] One such inhibitor has been identified and kinetically characterized in parallel with the pan-Class I HDAC inhibitor, SAHA.

MATERIALS AND METHODS

Recombinant HDAC. Carboxy-terminal FLAG-tagged human HDAC1 was stably expressed in HEK293F cells and affinity purified using an anti-Flag antibody matrix.

HDAC Activity Assay and IC_{50} Determination. These are described in Hamblett et al. [9]

***K_i* Determination from Activity Assay.** The HDAC reaction described in Hamblett et al. [9] was run as a 650 μL reaction where 50 μL aliquots were removed at sequential time points and added to development solution. The reaction was initiated with the addition of HDAC to 0.31 nM. The curve-fitting program Prism was used to fit all data to the given equations (vide infra).[17] The product formation rates were determined for a matrix of varying substrate and compound concentrations using either:

$$v = \frac{V_m}{1 + \frac{K_m}{S}\left[1 + \frac{I}{K_i}\right]} \quad (1)$$

for a competitive inhibitor following Michaelis–Menten assumptions (SAHA, fSAHA); or for inhibitors giving a curvilinear response (DW2a, fDW2a):

$$P = V_s t + \frac{(V_i - V_s)(1-\gamma)}{k_{obs}\gamma} \ln\left[\frac{1 - \gamma\exp(k_{obs}t)}{1-\gamma}\right] \quad (2)$$

where $\gamma = ([E])/([I])(1 - (V_s)/(V_i))^2$, V_i is the initial velocity, and V_s the steady-state velocity.

To determine the values for k_F, k_R, and K_i^{app} at each concentration of HDAC inhibitor, eq 3 was used:

$$k_{obs} = k_R + \left\{\frac{k_F}{1 + \frac{K_i^{app}}{[I]}}\right\} \quad (3)$$

The replot of the ratio of V_i (or V_s) to V_0 vs inhibitor concentration to eq 4 or eq 5 can be fit to a four-parameter logistic curve. The inflection point gives the K_i^{app} or K_i^{*app} for eqs 4 and 5, respectively.

$$\frac{V_i}{V_0} = \frac{1}{1 + \frac{I}{K_i^{app}}} \quad (4)$$

$$\frac{V_s}{V_0} = \frac{1}{1 + \frac{I}{K_i^{*app}}} \quad (5)$$

To determine the actual K_i and K_i^* from the IC_{50}, the Cheng–Prusoff conversion for a competitive inhibitor was used.[16]

To determine the fast k_{on} step, the definition of K_i was used:

$$K_i = \frac{k_{off}}{k_{on}} \quad (6)$$

Reversibility Determinations. The HDAC activity assay described in Hamblett et al. [9] was modified such that four sample types were conducted for each experiment: "diluted" and "undiluted" for both DMSO control and compound inhibition. In a volume of 10 μL, HDAC1 (618 nM) was incubated with compound (1 μM) or DMSO at 22 °C for 0 ("diluted") or 2 ("undiluted") hours; after the incubation, 1.99 mL of assay buffer was added to each sample. Immediately, after the dilution of the "undiluted" samples, 10 μL was added to 40 μL substrate, the plates were incubated at 37 °C, sample reactions were stopped at successive time points, and the fluorescence was read.

The rate of activity of the inhibitor "diluted" sample was used to define the expected steady-state rate (V_s) for the inhibited "undiluted" sample. This calculated value was used in eq 2 to determine k_{obs} and V_i.

Fluorescence Polarization Binding Assays. The assays were run in black, flat-bottomed, 96-well plates with the final assay buffer conditions of: 20 mM Hepes, pH 8.0, 137 mM NaCl, 2.7 mM KCl, 1 mM $MgCl_2$, and 0.01% v/v TritonX-100. Binding of HDAC to the fluorescent derivatives was followed by fluorescence polarization at Ex 485 nm/Em 530 nm. Either 2.5 nM fSAHA or 7.5 nM fDW2a was used as ligands for HDAC binding.

Association Assay of the FITC Compounds. To determine the kinetic and K_d values of the fluorescent derivatives to HDAC1, association of the labeled ligand to varying concentrations of HDAC1 (5 to 200 nM) was followed for at least 2 h. The data were fit to eq 7[10] that accounts for ligand depletion.

$$A = A_f + (A_b - A_f) \times \left[\frac{(L_T + K_d + R_T) - \sqrt{(L_T + K_d + R_T)^2 - 4L_T R_T}}{2L_T}\right] \quad (7)$$

where A is the anisotropy of the sample, A_f the anisotropy for totally free ligand, A_b the anisotropy for totally bound ligand, L_T the total ligand concentration, and R_T the total receptor concentration.

These calculated apparent K_d values were then plotted vs time and fit to either a single-exponential curve (fSAHA) or a double-exponential curve (fDW2a). The value at the plateau was the equilibrium affinity constant.

To determine the association rates, the bound ligand calculated from the anisotropy data (vide supra) was plotted vs time. The data were fit to an exponential curve to determine $k_{obs}{}^a$. These values were replotted vs HDAC1 concentration and fit to:

$$k_{obs}^a = k_{on}[\mathrm{HDAC}] + k_{off} \quad (8)$$

to determine $k_{on}{}^a$ and $k_{off}{}^a$.

***k_{off}* Determination for the FITC-Compounds.** FITC-labeled compound (2.5 nM) was preincubated with HDAC (5–300 nM) for at least 3 h at RT, after which unlabeled SAHA was added to a final concentration of 10 μM to displace the labeled compound. Sequential reads were performed following

dx.doi.org/10.1021/bi400936h | Biochemistry 2014, 53, 725–734

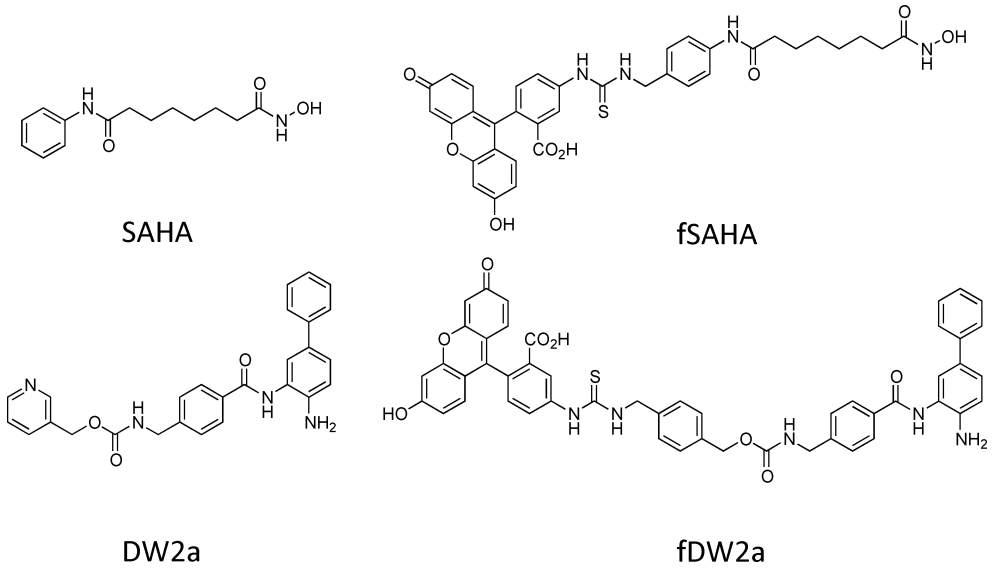

Figure 1. HDAC inhibitors used for kinetic and binding studies. Both the hydroxymate (SAHA) and the biaryl (DW2a) were conjugated to FITC (fSAHA and fDW2a, respectively) for use in fluorescence polarization binding studies. Detailed synthesis protocols can be found in the Supporting Information (SI) Supplemental Method S1).

the fluorescence polarization, and the results plotted to an exponential decay to determine the off-rate.

K_i Determination for Unlabeled Compounds. Using the protocol for determining k_{off} values, the IP values of unlabeled compounds were determined over 3 h and replotted vs time. fSAHA bound to HDAC was calculated using eq 7, plotted vs HDACi concentration, and a four-parameter logistic fit was applied to the data to determine the IC_{50} values. These IC_{50}'s were transformed to K_i^{app} using eq 9, taking into consideration ligand and receptor depletion,[11] replotted vs time, and the data fit to an exponential decay. The plateau value of this decay gave the steady-state K_i.

$$K_i = \frac{IC_{50}}{Y_0 + 1 + \frac{L_T(Y_0+2)}{2K_d(Y_0+1)}} - K_d\left(\frac{Y_0}{Y_0+2}\right) \quad (9)$$

where Y_0 is the initial bound/free ratio of fSAHA, and K_d refers to the dissociation constant of fSAHA to HDAC1.

Only SAHA could be fit to a single-phase exponential decay curve that would be expected for a simple association−dissociation equilibrium. A two-phase exponential decay curve had to be used to fit the DW2a data, indicating a more complicated series of events was occurring during unlabeled compound binding. The steady-state K_i value in this case is actually K_i*.

Modeling. A homology model of human HDAC1 was constructed using Amber8 and a version of the parm94 biomolecular force field extended to organic small molecules. The model was prepared using the OPLS force field and the protein preparation tools in the Schrödinger software suite. DW2a was then docked using Glide. Molecular Dynamics studies were performed and analyzed using Desmond. The HDAC1-DW2a model was subjected to a 2 ns simulation at a constant temperature of 300 K, and analysis of the geometries of protein and ligand indicated the stability of the system.

RESULTS

Potency and Selectivity of a Novel HDAC Inhibitor. To identify HDAC1/2-specific inhibitors, compounds were screened using a modified commercial HDAC activity assay to inhibit the deacetylation of a synthetic peptide.[9] Several such compounds were identified, and one was selected for further characterization. In contrast to SAHA, which inhibits HDACs 1, 2, 3, and 6 with IC_{50} values from 40 to 100 nM, DW2a is a potent HDAC1/2 inhibitor (IC_{50} values 10 nM and 72 nM, respectively) that shows 1000-fold less selectivity for HDACs 3 or 6.[15] Inhibitor chemical structures are presented in Figure 1.

Mechanism of Inhibition. To define and compare the mode of inhibition of SAHA and DW2a, progress curves of HDACs with varying amounts of substrate and HDAC inhibitor were acquired. Classical Michaelis−Menten kinetics was used to fit the data. The K_m in the absence of inhibitor was determined to be 26 μM, and the k_{cat} value, 3.6 s^{-1}.

Parts A and B of Figure 2 show representative progress curves with HDAC1 and increasing concentrations of the two HDAC inhibitors. HDAC1 inhibited by SAHA exhibited the linear initial velocities necessary for utilizing Michaelis−Menten assumptions (Figure 2A), whereas DW2a-inhibited reactions did not (Figure 2B). In order to determine the K_i value, the linear initial velocities were replotted vs the substrate concentration at various SAHA concentrations and fit to eq 1. Competitive inhibition is the preferred model (Figure 2E), as the data did not fit to the equations describing other modes of inhibition. The K_i value was determined to be 16 nM, similar to its determined IC_{50} value.[15]

Time-Dependence of HDACi's. One of the assumptions of Michaelis−Menten kinetics is that the various enzyme complexes with substrate and/or inhibitor come to equilibrium rapidly. To test if this assumption no longer holds for DW2a, HDAC1 was preincubated with inhibitor up to 4 h prior to running the activity assay (Table 1). As could be predicted by the linear progress curves in the presence of SAHA, the IC_{50} values for SAHA were maintained at ~40 nM, regardless of incubation time. Those of DW2a declined over 4 h by approximately 8-fold when preincubated with HDAC1, indicating a slow step in the binding of compound to enzyme.

Mechanisms Leading to Slow-Binding Inhibition. Several mechanisms can lead to slow-type inhibition (reviewed

dx.doi.org/10.1021/bi400936h | Biochemistry 2014, 53, 725−734

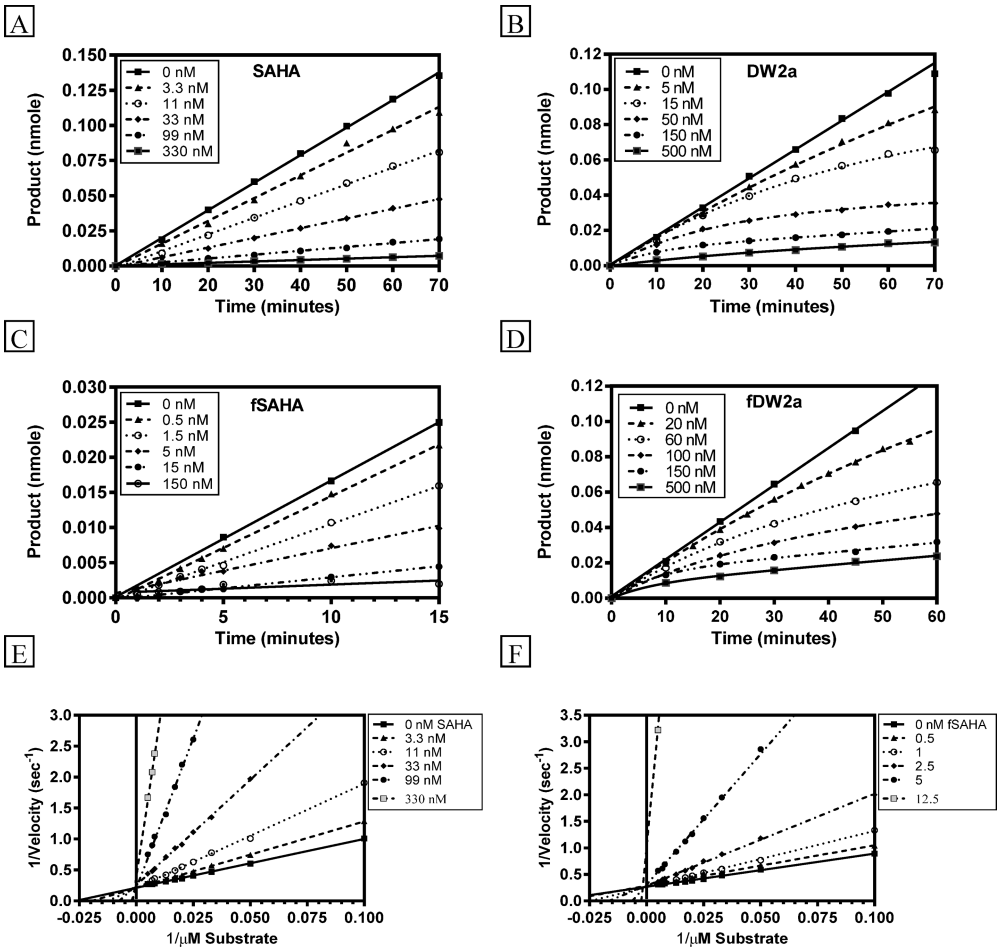

Figure 2. Potency and mechanism of action of HDAC inhibitors for HDAC1. (A–D) Product formation of HDAC1-catalyzed deacetylase reactions at increasing concentrations of HDAC inhibitors at 30 μM substrate. (A): SAHA; (B): DW2a; (C): fSAHA; (D): fDW2a). (E and F): Lineweaver–Burke replots of the rates of product formation at the individual substrate and HDAC inhibitor concentrations of A and C, respectively. The K_m was determined to be 26 μM and the k_{cat} value 3.6 s^{-1}; the average K_i values were determined to be 15.9 ± 3.6 (SAHA) and 1.5 ± 0.5 (fSAHA).

Table 1. Effect of Preincubation of HDAC1 with HDAC Inhibitors on the in Vitro Potency[a]

	mean IC_{50} ± SEM (nM)		
	0 h	1 h	4 h
SAHA	32 ± 6	33 ± 4	46 ± 4
fSAHA	5.0 ± 0.0	5.0 ± 0.5	7.0 ± 1.0
DW2a	15 ± 2	5.0 ± 0.2	2.0 ± 0.4
fDW2a	61 ± 8	24 ± 3	13 ± 1

[a]Reactions were initiated by addition of substrate to 0.31 nM HDAC1 preincubated with varying concentrations of HDAC inhibitor for 0–4 h. Each IC_{50} value was determined a minimum of four times.

by Copeland[17]). The two simplest mechanisms involve either slow irreversible binding or a simple equilibrium containing a slow on-rate. More complicated mechanisms involve a conformational change of the low affinity enzyme–inhibitor encounter complex or of the unbound enzyme or inhibitor prior to the binding event. Although the last mechanism has been proposed to explain the slow-binding kinetics of HDAC2 inhibition for an alternate benzamide HDAC inhibitor,[16] such conformational changes rarely occur with small-molecular weight ligands.[17]

The HDAC Inhibitors Reversibly Bind HDAC1. To address the reversibility of DW2a-binding, activity assays of HDAC1 preincubated with HDAC inhibitor were performed. HDAC1 (0.6 μM) was incubated with 1 μM compound and then diluted either immediately upon creating the mixture (t = −2 h) or after 2 h (t = 0). This dilution was such that the HDAC inhibitor concentration fell from at least 100-fold above to at least 5-fold below its IC_{50} value. The activity assay was initiated at t = 0 and product formation monitored for 4 h. As can be seen in Figure 3A, the rate of product formation in the presence of SAHA did not differ regardless of its time of dilution, suggesting reversible binding with a rapid off-rate (k_{off}^{Rev} > 0.23 min^{-1}). In contrast, DW2a, while also demonstrating reversible inhibition (Figure 3C), exhibited a slow off-rate (k_{off}^{Rev} of 0.0086 min^{-1}). Here the rate of product formation for the reaction mixture diluted at t = 0 took over 4 h before it reached the rate of the mixture diluted 2 h prior, consistent with a slow-binding model (eq 2).

Comparison of the Two Reversible Binding Mechanisms. The nonlinear velocity curves for DW2a in Figure 2 contain two components: a burst of product formed (V_i) followed by the steady-state rate of product formation (V_s). To determine k_{obs}, the data were fit to eq 2. By plotting these k_{obs} values against the HDACi concentration (Figure 4A), one can distinguish between the mechanisms with a slow binding step or with a slow conformation change.[17] The lack of linearity indicated that DW2a binding involves a conformational change;

dx.doi.org/10.1021/bi400936h | Biochemistry 2014, 53, 725–734

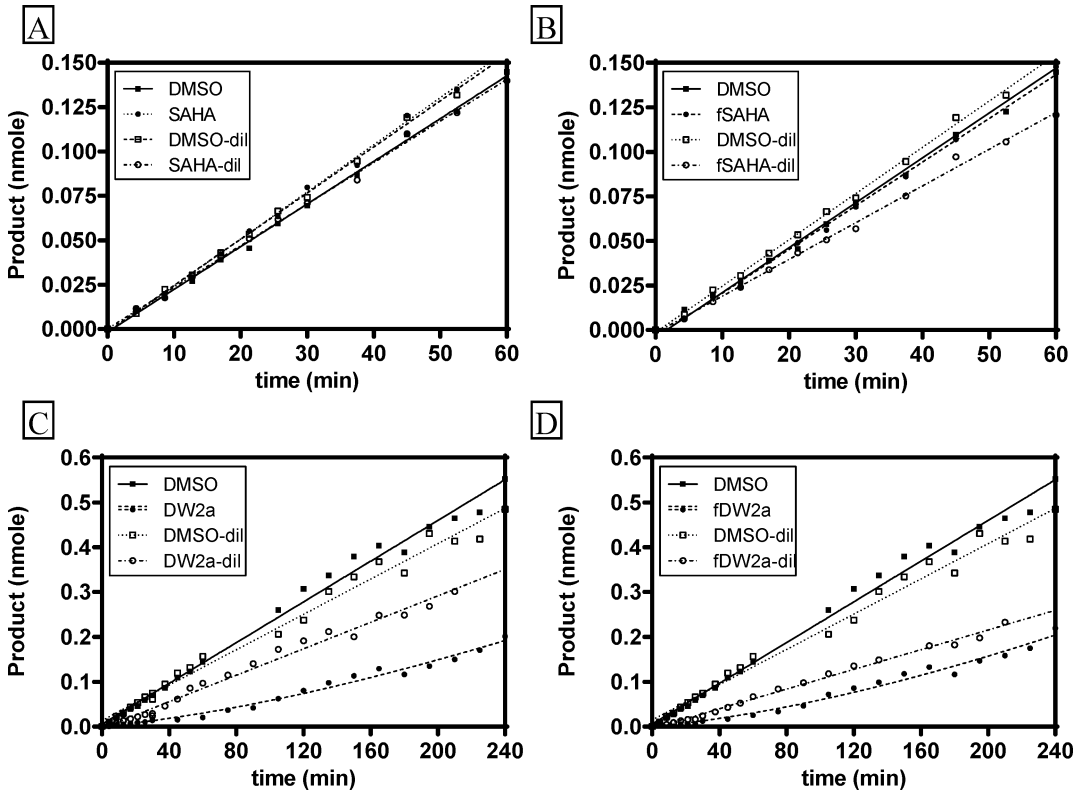

Figure 3. HDAC inhibitors bind reversibly to HDAC1. HDAC1 was incubated with HDAC inhibitors prior to initiating the activity assay ($t = 0$). The samples labeled "dil" were diluted 2 h prior to $t = 0$ to define the inhibition found at equilibrium; the remaining samples were diluted at $t = 0$. Both the unlabeled and labeled SAHA dissociated quickly with complete dissociation seen at the earliest time point (4.3 min) giving a k_{off} of >0.23 min^{-1} for both SAHA and fSAHA. The DW2a variants reached the equilibrium rate in more than 1 h. The k_{off} values were determined to be 0.0086 min^{-1} and 0.0098 min^{-1} for DW2a and fDW2a, respectively.

the hyperbolic shape of the curve reflects the permutation where the initial enzyme−inhibitor encounter complex changes conformation to a tighter binding form as illustrated in Figure 5.

Biaryl HDAC Inhibitors Are Competitive with Substrate. Due to the slow-binding kinetics of the biaryl HDAC inhibitors, the replot of velocity vs substrate concentration cannot be used to determine the mechanism of inhibition as with the hydroxamate class. Rather, the plot of k_{obs} vs the ratio of substrate concentration to the K_m can be used [17] (Figure 4B). These data fit a declining hyperbola, characteristic of a competitive mechanism.

Determining Kinetic Constants for the Biaryl HDAC Inhibitors Using a Slow-Binding Model. As the mechanism of action was determined to involve a conformational change, other kinetic constants could be determined using the values of k_{obs}, V_i, and V_s as described by eq 2. k_{obs} is a function of the rates of conformational change (k_F and k_R) and the affinity of the initial encounter complex as defined by eq 3. k_F, k_R, and K_i^{app} could be determined from plotting k_{obs} vs the HDACi concentration (Figure 4A). The k_R value for DW2a was found to be at least 1000-fold slower than the k_{off} of SAHA. When the initial and steady-state velocities (V_i and V_s, respectively) were plotted as ratios to the uninhibited velocity vs the concentration of HDACi, the K_i and K_i* values could be derived (eqs 4 and 5) (Figures 6A and 6B). The apparent affinity constant (K_i^{app}) was then converted to the actual affinity constant (K_i) via the Cheng−Prusoff equation for competitive inhibitors [18] (Table 2).

Design of an Assay To Directly Follow Binding and Dissociation. To further investigate the slow-binding phenomenon of DW2a, a fluorescence polarization (FP)-based binding assay was developed using fluorescein-labeled analogues of the two inhibitors (Figure 1). To ensure that the addition of this fluorescein moiety had not changed the mechanisms of inhibition, the inhibitory characteristics and potency were compared to the unlabeled compounds. Although addition of the fluorescein had some effect on the potency (Table 1), there was no effect on the linearity, or lack thereof, of the velocity curves (Figure 2C and D). FITC-SAHA (fSAHA) is a competitive (Figure 2F) and reversible inhibitor (Figure 3B) with a K_i value of 1.5 nM. As with the parental compound, the FITC-labeled DW2a (fDW2a) exhibited time-dependent potency (Table 1) and kinetics (Figure 2D), reversible and competitive inhibition (Figures 3D and 4B), and underwent a conformational change at the initial encounter complex (Figure 4A). Thus, the addition of the fluorescein did not change the mechanistic properties of the parental compounds.

Determination of the On- and Off-Rates of the FITC-Labeled Compounds. Association of the labeled HDAC inhibitors was tracked by fluorescence polarization at different HDAC1 concentrations until equilibrium was achieved (Figures 7A and 7B). To determine the association rate constant k_{obs}^{a}, the data were fit to a single exponential curve for each of the different HDAC1 concentrations. The k_{obs}^{a} values for fSAHA may be underestimated because an insufficient number of early points could be obtained to confidently describe the curves. A replot of k_{obs}^{a} vs HDAC concentration (Figure 7C) yielded values for k_{on}^{a} (the slope) and k_{off}^{a} (y-intercept) (eq 8). The k_{on}^{a} values derived from these plots showed that association to HDAC1 was at least 40-fold slower for fDW2a than for fSAHA. The extrapolated k_{off}^{a} for fSAHA was at least 61-fold faster

dx.doi.org/10.1021/bi400936h | *Biochemistry* 2014, 53, 725−734

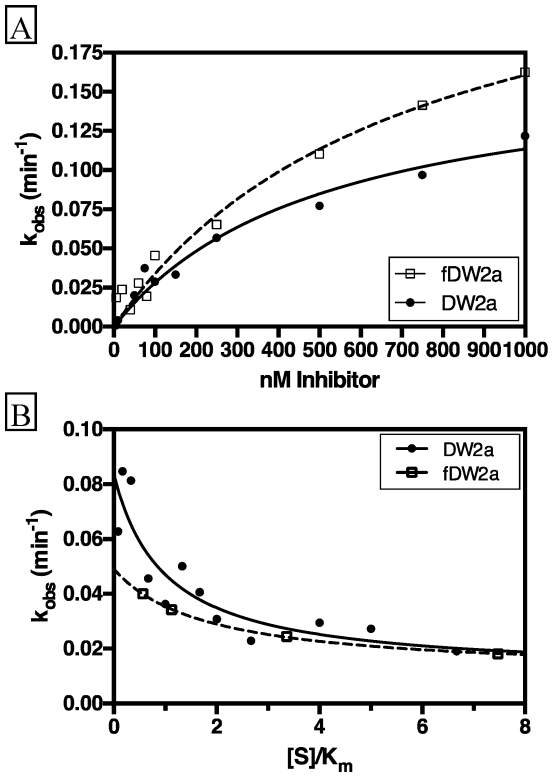

Figure 4. Biaryl HDAC inhibitors are competitive inhibitors that induce a conformational change upon binding HDAC. (A) k_{obs} values from the activity assays were plotted vs the HDAC inhibitor concentration to determine the binding mode. The hyperbolic curve indicates that these inhibitors induce a conformational change after the initial binding complex is formed. (B) Representative replot of the k_{obs} values in the presence of HDACi at varying substrate concentrations demonstrates that the inhibitors are competitive with substrate binding.

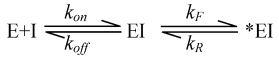

Figure 5. Schematic of the two-step binding performed by the biaryl HDAC inhibitors and the associated rate constants. In order for slow-type inhibition to be observed, the on- and off-rates (k_{on} and k_{off}, respectively) must be fast in comparison to the forward (k_F) and reverse (k_R) rates of conformational change; the reverse rate must be significantly slower than the other three rates. Note that in such a case, the observed off-rate is k_R rather than reflecting the true k_{off}.

(1.23 min^{-1}) than that of fDW2a whose k_{off}[a] was too low to be determined accurately by this method (<0.02 min^{-1}).

From this same data set, the K_d^{app} at successive time points could be determined by plotting bound inhibitor vs total HDAC1. Replotting K_d^{app} vs time gave an exponential change in K_d^{app} where the equilibrium affinity could be determined from the plateau (Figure 7D). The equilibrium affinity was 6.8 nM (K_d) for fSAHA and 3.1 nM (K_d*) for fDW2a.

Determination of the Off-Rates of the FITC-Labeled Compounds by Dissociation Kinetics. To directly measure the off-rates of fSAHA and fDW2a, an excess of unlabeled SAHA was added to the equilibrated HDAC1·FITC-inhibitor mixture, and the loss of binding was measured over time. SAHA was used as it demonstrated fast kinetics and at high excess is expected to prevent rebinding of the labeled compounds. fSAHA dissociation was rapid (0.51 min^{-1}) and more than 1000-fold faster than that of fDW2a (2.5 × 10^{-5} min^{-1}) (Figure 8).

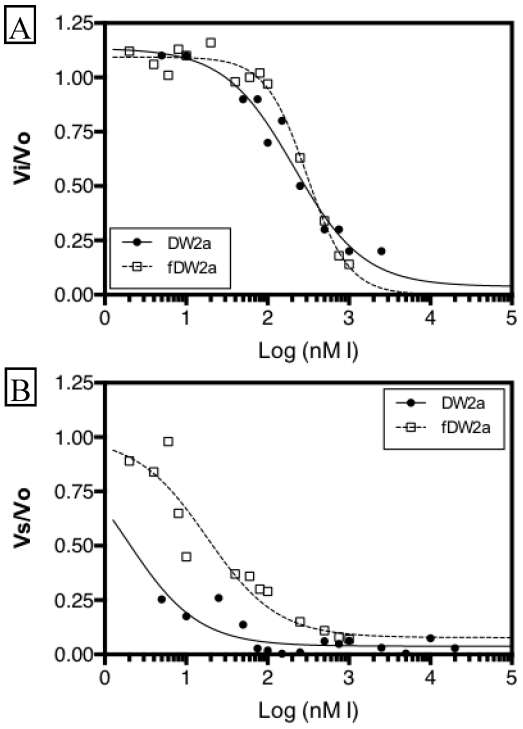

Figure 6. Determination of the affinities of the initial encounter complex and the conformationally changed complex. Representative replots of the (A) initial or (B) steady-state velocity as a fraction of the uninhibited velocity vs the biaryl concentration gave the apparent affinity constants K_i^{app} and K_i*^{app}, respectively.

Characterization of the Unlabeled Compounds. The unlabeled inhibitors were titrated and added to the pre-incubated fSAHA·HDAC1 complex. The K_i^{app} values were determined (eq 9) at successive time points and plotted vs time (Figure 9). At equilibrium, the K_i^{app} values approached the true affinity constants. The K_i^{app} values for SAHA reached equilibrium more rapidly than could be measured, whereas those for DW2a took at least 30 min to reach equilibrium and required a two-phase exponential fit to describe the data. K_i values for SAHA (13 nM) agreed with that determined by the kinetic analysis (vide supra). The K_i^{app} value for DW2a at equilibrium (0.7 nM) reflects the high affinity dissociation constant (K_i*).

DISCUSSION

There has been much discussion of the potential merits for selectively inhibiting HDACs 1 and 2 for the treatment of cancer rather than the current use of relatively unselective inhibitors such as SAHA and LBH589. It has been hypothesized that there could be increased tolerability through the use of more selective inhibitors. In the course of identifying such a selective inhibitor, we identified a family of biaryls that gave us the opportunity to examine such putative advantages.[15] In these studies, DW2a, one example of this family, has been enzymatically characterized and compared to SAHA (summarized in Table 2).

It has previously been demonstrated that HDACs 1 and 2 conform to Michaelis−Menten assumptions when measuring the rate of product formation.[21] Although the substrate and assay methodology used by Schultz et al. and Chou et al. was different than that used in this paper, the K_m and V_{max} values determined here are similar in scale and conform to the Michaelis−Menten kinetic model.

dx.doi.org/10.1021/bi400936h | Biochemistry 2014, 53, 725−734

Table 2. Summary of All Rate and Binding Constants[a]

	SAHA	fSAHA	DW2a	fDW2a	derivation
k_{off}^{Rev} (min^{-1})	>0.23[b]	>0.23[b]	0.0086 ± 0.0029[c]	0.0098 ± 0.0055[c]	reversibility[d]
k_{off}^{a} (min^{-1})	ND	1.2 ± 0.4[b]	ND	<0.02[c]	association
k_{off}^{d} (min^{-1})	ND	0.521 ± 0.019[b]	ND	(2.5 ± 0.8) × 10^{-5}[c]	dissociation
k_{R}^{Act} (min^{-1})	ND	ND	0.00017 ± 0.0002[b]	0.00085 ± 0.0005[b]	activity assay
k_{off} (min^{-1})	ND	ND	ND	0.75[b]	calcd from $K_i \times k_{on}^{a}$
k_{on}^{a} ($M^{-1}min^{-1}$)	ND	(2.0 ± 0.4) × 10^8	ND	(4.7 ± 0.3) × 10^6	association
k_{on} ($M^{-1}min^{-1}$)	>1.4 × 10^7	>1.5 × 10^8	ND	ND	calcd from $k_{on} = k_{off}^{Rev}/K_i$
K_d (nM)	ND	6.2	ND	ND	calcd from $K_d = k_{off}^{a}/k_{on}^{a}$
equilibrium affinity constant (nM)	13 ± 1 (K_i)	6.8 ± 0.8 (K_d)	1.1 ± 0.3 (K_i*)	3.1 ± 0.9 (K_d*)	binding assay: change of K_i or K_d with time
K_i (nM)	15.9 ± 3.6[e]	1.5 ± 0.5[e]	161 ± 45[f]	159 ± 23[f]	activity assay
K_i* (nM)	NA	NA	<0.9	<0.7	calcd from V_s/V_0[d]
k_F (min^{-1})	NA	NA	0.054 ± 0.005	0.058 ± 0.005	calcd from k_{obs} vs [I][d]

[a]The average ± SEM of the various affinity and rate constants were determined by the indicated calculations or experiments. Each experiment was performed a minimum of three times. Lettered superscripts in the first column distinguish the source of the measured rates. NA: not applicable; ND: not determined. Italic superscripts in the data columns refer to the source of the data. [b]Value represents the rate of the inhibitor dissociating from HDAC1. [c]Value represents the reverse conformational change (k_R). [d]Data acquired from activity assays. [e]Michaelis–Menten competition model (activity assay); [f]Calculated from V_i/V_0 (activity assay).

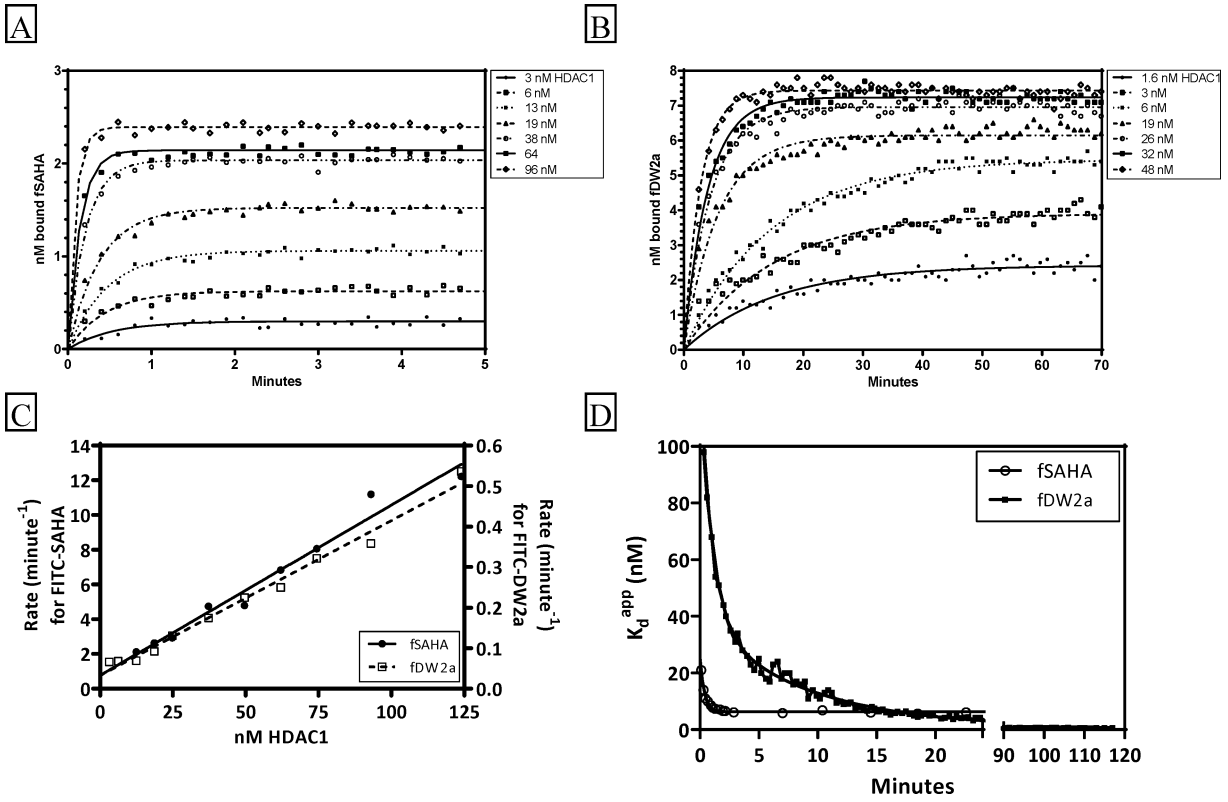

Figure 7. Association kinetics of FITC-labeled HDAC inhibitors. (A and B) Binding to HDAC1 was initiated by addition of fHDACi and was followed by fluorescence polarization. (A) fSAHA. (B) fDW2a. (C) k_{obs} values from A and B were replotted vs HDAC1 concentration to determine the on-rate (k_{on}^{a}) from the slope and the off-rate (k_{off}^{a}) from the *y*-intercept. (D) K_d^{app} was plotted vs time to determine the equilibrium affinity constant. fSAHA and fDW2a were fit to a one- or two-phase exponential curve, respectively.

Characterization of SAHA and its FITC-labeled analogue by activity assays demonstrated that they both come rapidly to equilibrium for inhibiting HDACs 1, 2, and 3 (Figure S1, SI). Our determined K_i value for SAHA of 16 nM agrees with that of Beckers et al. (14 nM) [22] and Chou et al. (5.4 nM).[20] The addition of fluorescein to SAHA had no impact on its mechanism of action or selectivity although it did improve the potency by 10-fold. Consistent with the observed rapid equilibrium, the off-rates measured for SAHA and fSAHA were >0.23 min^{-1} and 0.521 min^{-1}, respectively. The binding assay defined an association rate constant for fSAHA as 2 × 10^8 M^{-1} min^{-1} and is likely to be diffusion limited. The calculated k_{on} value for SAHA was >1.4 × 10^7 min^{-1} M^{-1}. Other HDAC inhibitors such as LBH589, HC Toxin, and PXD101 also follow these fast binding kinetics and are competitive inhibitors (data not shown).

Unlike the hydroxamate class to which SAHA belongs, members of the biaryl family such as DW2a and fDW2a have displayed slow binding characteristics as demonstrated by IC_{50} dependence on preincubation time (Table 1). The clinical compound MS275 also demonstrates moderate slow binding (data not shown). The slow establishment of equilibrium explains the nonlinear progress curves and necessitated the use

dx.doi.org/10.1021/bi400936h | *Biochemistry* 2014, 53, 725–734

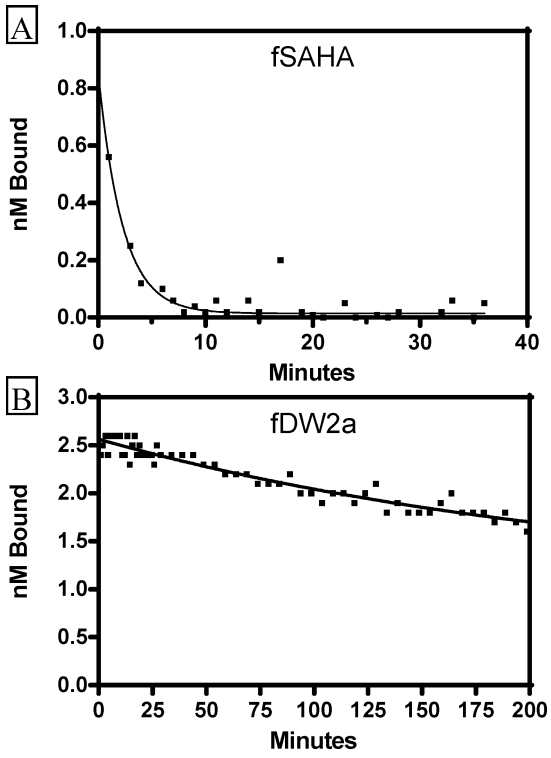

Figure 8. Dissociation kinetics of FITC-labeled HDAC inhibitors. Dissociation was initiated by addition of SAHA to preincubated HDAC1·fHDACi. (A) fSAHA. (B) fDW2a. Bound fHDACi was measured by fluorescence polarization. Representative curves at a single HDAC1 concentration are shown.

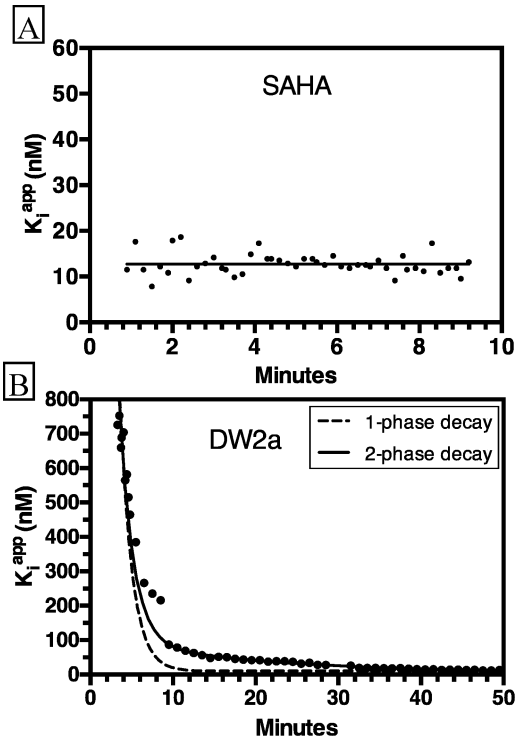

Figure 9. Affinity constant determination of unlabeled HDAC inhibitors to HDAC1. Competition experiments were performed by adding unlabeled HDACi to preincubated HDAC1·fSAHA. K_i^{app} values were determined at successive time points and replotted vs time. The plateau value reflects the true affinity constant where $K_i = k_{off}/k_{on}$ for SAHA (8A) or $K_i^* = K_i/[1 + (k_F/k_R)]$ for DW2a (8B). The replot of apparent dissociation constants for DW2a vs time were fit to both one- and two-phase exponential decays illustrating the biphasic association character of DW2a binding.

of non-Michaelis–Menten analyses to define affinities and mechanism. This characteristic was recapitulated in the binding assays. Several assays helped to distinguish which mechanism of slow binding was used by these biaryl compounds. Using both activity and binding assays, it was demonstrated that DW2a binds reversibly and exhibits dissociation kinetics of less than 0.0001 min^{-1}, more than 1000-fold slower than fSAHA.

The rate for the reverse conformational change (k_R) as determined by the reversibility activity assay may be overstated for DW2a. Although the 1000-fold compound dilution went below the IC_{50} values, considerable inhibition remained with DW2a, suggesting that the equilibrium dissociation constant (K_i^*) is lower than expected. On the basis of the curvature of the data fit, DW2a may not have reached equilibrium during the course of this experiment. As the various assay protocols were nearing the lower limit of enzyme and ligand concentrations that could be reliably used, it is quite possible that these concentrations limited precise measurement of K_i^* and k_R for DW2a. Supporting this, the binding experiment values for k_{off}[d] were at least 10-fold lower than those derived from the reversibility assay.

The proposed mechanism includes a conformational change that occurs after the enzyme–ligand complex forms. An analogous mechanism where a conformational change of the enzyme is required to bind the inhibitor was eliminated by the k_{obs} vs HDAC inhibitor concentration replot (Figure 4A); k_{obs} would have decreased rather than increased in this scenario.[17] Replots of the kinetic k_{obs} values provide confirmation that the biaryls are competitive inhibitors, supported by the binding assays where both DW2a compounds could compete for binding with the two SAHA compounds.

In order to determine the actual k_{off} for fDW2a, eq 6 was applied. As the binding assay measured the concentrations of both conformations of the bound enzyme complex, the plot of k_{obs}[a] vs HDAC1 enzyme concentration (Figure 7C) was linear rather than the expected hyperbola, indicating that the on-rate reflects the rate of association rather than the rate of conformational change in the forward direction. This on-rate was about 40-fold slower than that of fSAHA. From the k_{on} and the K_i values, the actual k_{off} was determined to be 0.75 min^{-1} which is similar to that of fSAHA, once again supporting the conclusion that it is the reversal of the putative conformational change that is slow.

On the basis of these various assays, it was evident that the biaryl inhibitors bind to the enzyme rapidly and reversibly involve a slow conformational change. Docking studies using a homology model of human HDAC1 suggested that the biaryl moiety of DW2a was likely to occupy a hydrophobic cavity denoted as the 'foot pocket', immediately adjacent to the catalytic zinc ion. (Figure 10) This foot pocket has also been modeled to explain the selectivity of the biaryl inhibitor class for HDAC1 over HDAC3.[23] A similar binding orientation has been determined experimentally in PDB entry 3MAX—the complex of HDAC2 with a biaryl benzamide. For HDAC2, a semiempirical QM study suggested the slow binding kinetics was associated with the disruption of an internal hydrogen bond.[16] We subjected our model of the initial recognition complex of HDAC1–DW2a to molecular dynamics and observed changes in the foot pocket region, consistent with an induced

dx.doi.org/10.1021/bi400936h | *Biochemistry* 2014, 53, 725–734

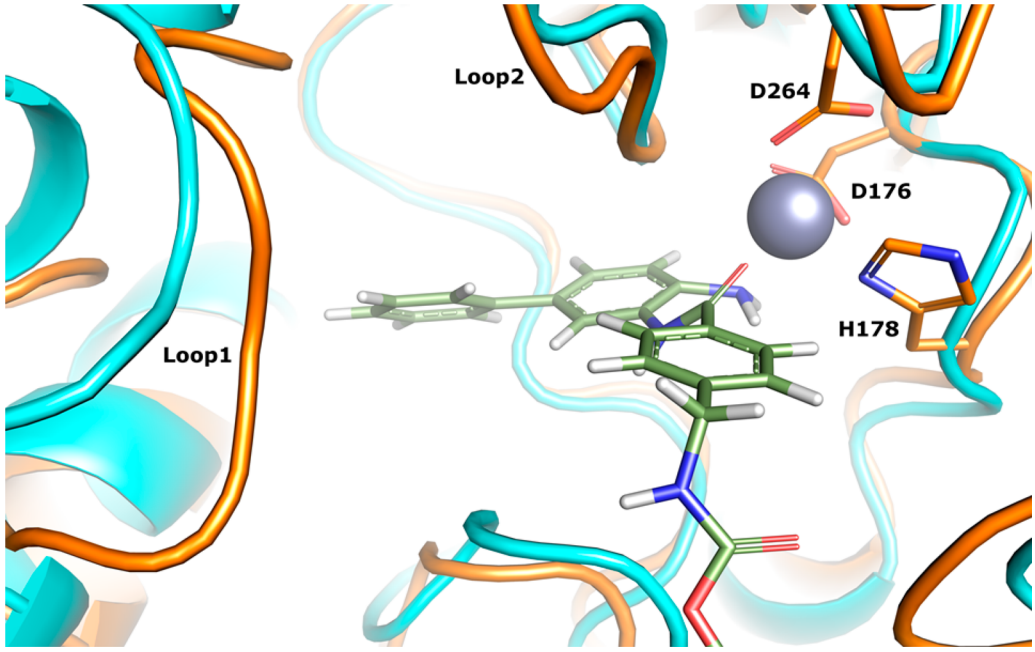

Figure 10. Model of a potential mechanism for the conformational change implied by the biaryl compound class kinetics. A representative complex of DW2a (green) with HDAC1 (orange) from the MD simulation, overlaid with the initial recognition complex (cyan). For clarity, DW2a, the zinc ion, and the coordinating residues Asp176, His178, and Asp264 are shown only for the MD structure. Zinc coordination by HDAC1 and DW2a was consistent with previous studies. [17] Analysis of MD trajectories indicated a concerted motion of Loop1 (between helices α1 and α2) and Loop2 (between sheet β8 and helix α10) toward DW2a, consistent with an induced fit of the biaryl moiety.

fit of DW2a, and propose that these conformational changes offer an alternate explanation for the slow binding kinetics of this ligand class. To support this explanation, studies with HDAC2 paralleled the results seen for HDAC1 (Figure S1, SI).

There are practical implications to utilizing slow-binding, tight inhibitors. These biaryl HDAC inhibitors could be predicted to have altered kinetics in cell-based and in vivo models. It would be supposed that the slow binding characteristic would make it possible for a less intensive dosing schedule and possibly fewer associated toxicities. Indeed, these predictions have been borne out (SI). Treatment of HCT116 cells with DW2a resulted in a dose- and time-dependent effect on cell proliferation. (Figure S2, SI) The kinetics of histone deacetylation and induction of apoptosis were fast for SAHA and delayed for DW2a, consistent with our biochemical analyses. Compound washout experiments resulted in a fast reversal of SAHA-induced effects, whereas the effects observed with DW2a were more persistent after compound washout (Figure S3, SI). SAHA and DW2a were used to treat xenograft tumor-bearing mice and were similarly efficacious. However, whereas SAHA required QD[24,25] dosing, DW2a yielded similar efficacy with less frequent (biweekly) dosing. Histone deacetylation required high plasma levels of SAHA to maintain its pharmacodynamic effects. DW2a, however, had prolonged effects on histone acetylation status despite its complete disappearance from the plasma (Figure S4, SI). These results have been recapitulated using another biaryl compound in both cells [21] and in vivo.[20] These results also support a longer $T_{1/2}$ than would be calculated from the k_{off}^{Rev} reported in Table 2. If the $T_{1/2}$ is at least 12 h as suggested by the washout experiments, k_R would be ~0.0001 min^{-1} and the equilibrium K_d* ≈ 100 pM. This correlates well to the K_d* and k_R values determined in the activity and binding assays, respectively. It further supports the conclusion that the k_{off}^{Rev} rate determined in the reversibility assay overstated the rate of the reverse conformational change. An alternative explanation for the longer than expected functional half-life in cells and mice could be slow compound transit through the plasma membrane and, thus, a prolonged exposure of HDAC to DW2a.

DW2a provides us with a tool to test the hypothesis that an HDAC1/2-specific inhibitor may offer a more efficacious and better tolerated alternative to pan-HDAC inhibitors in cancer patients.

■ ASSOCIATED CONTENT

Supporting Information

Chemical synthesis of the FITC analogues, cell-based assays, and mouse xenograft efficacy data. This material is available free of charge via the Internet at http://pubs.acs.org.

■ AUTHOR INFORMATION

Corresponding Author

*Telephone: 781-839-4896. E-mail: kral@alum.mit.edu.

Present Addresses

[¶]AstraZeneca, 35 Gatehouse Drive, Waltham, MA 02451.
[†]Reynolds & Reynolds, 200 Quality Circle, College Station, TX 77845.
[‡]Ironwood Pharmaceuticals, 301 Binney St., Cambridge, MA 02142.
[#]Translational Research Program, Boston Children's Hospital, 2 Avenue Louis Pasteur, Boston, MA 02115.
[§]Medicinal Chemistry, Amgen, Inc., One Amgen Center Drive, Thousand Oaks, CA 91320.
[∥]AstraZeneca - Oncology iMed, 35 Gatehouse Dr., Waltham, MA 02451.
[⊥]Harvard School of Public Health, 665 Longwood Ave., Boston, MA 02115.

Notes

The authors declare no competing financial interest.

■ ABBREVIATIONS

APC, Adenomatous Polyposis Coli; CCR2, CC chemokine receptor 2; fDW2a, FITC-labeled DW2a; ER, Estrogen Receptor; FP, Fluorescence Polarization; fSAHA, FITC-labeled SAHA; HAT, Histone Acetyl Transferase; HDAC, Histone Deacetylase; HDACi, HDAC Inhibitor; MS275, *N*-[[4-[[(2-Aminophenyl)amino]carbonyl]phenyl]methyl]-3-pyridinylmethyl Ester, Carbamic Acid; OPLS, Optimized Potentials for Liquid Simulations; SAHA, Suberoylanilide Hydroxamic Acid

■ REFERENCES

(1) Reviewed in Witt, O., Deubzer, H. E., Milde, T., and Oehme, I. (2009) HDAC Family: What are the Cancer Relevant Targets? *Cancer Lett. 277*, p8−21.

(2) Suzuki, T., Yokozaki, H., Kuniyasu, H., Hayashi, K., Naka, K., Ono, S., and Ishikawa, T. (2000) Effect of Trichostatin A on Cell Growth and Expression of Cell Cycle- and Apoptosis-Related Molecules in Human Gastric and Oral Carcinoma Cell Lines. *Int. J. Cancer 88*, 992−997.

(3) Curtin, M., and Glaser, K. (2003) Histone Deacetylase Inhibitors: The Abbott Experience. *Curr. Med. Chem. 22*, 2373−2392.

(4) Choi, J. H., Kwon, H. J., Yoon, B. I., Kim, J. H., Han, S. U., Joo, H. J., and Kim, D. Y. (2001) Expression Profile of Histone Deacetylase 1 in Gastric Cancer Tissues. *Jpn. J. Cancer Res. 92*, 1300−1304.

(5) Zhu, P., Martin, E., Mengwasser, J., Schlag, P., Janssen, K. P., and Göttlicher, M. (2004) Induction of HDAC2 Expression upon Loss of APC in Colorectal Tumorigenesis. *Cancer Cell. 5*, 455−463. Krishnan, M., Singh, A. B., Smith, J. J., Sharma, A., Chen, X., Eschrich, S., Yeatman, T. J., Beauchamp, R. D., and Dhawan, P. (2010) HDAC Inhibitors Regulate Claudin-1 Expression in Colon Cancer Cells through Modulation of mRNA Stability. *Oncogene 29*, 305−312.

(6) Zimmermann, S., Kiefer, F., Prudenziati, M., Spiller, C., Hansen, J., Floss, T., Wurst, W., Minucci, S., and Göttlicher, M. (2007) Reduced Body Size and Decreased Intestinal Tumor Rates in HDAC2-Mutant Mice. *Cancer Res. 67*, 9047−54.

(7) Bicaku, E., Marchion, D. C., Schmitt, M. L., and Münster, P. N. (2008) Selective Inhibition of Histone Deacetylase 2 Silences Progesterone Receptor-Mediated Signaling. *Cancer Res. 68*, 1513−1519.

(8) Reviewed in Karagiannis, T. C., and El-Osta, A. (2007) Will Broad-Spectrum Histone Deacetylase Inhibitors Be Superseded by More Specific Compounds? *Leukemia 21*, 61−65.

(9) Hamblett, C. L., Methot, J. L., Mampreian, D. M., Sloman, D. L., Stanton, M. G., Kral, A. M., Fleming, J. C., Cruz, J. C., Chenard, M., Ozerova, N., Hitz, A. M., Wang, H., Deshmukh, S. V., Nazef, N., Harsch, A., Hughes, B., Dahlberg, W. K., Szewczak, A. A., Middleton, R. E., Mosley, R. T., Secrist, J. P., and Miller, T. A. (2007) The Discovery of 6-Amino Nicotinamides As Potent and Selective Histone Deacetylase Inhibitors. *Bioorg. Med. Chem. Lett. 17*, 5300−5309.

(10) Swillens, S. (1995) Interpretation of Binding Curves Obtained with High Receptor Concentrations: Practical Aid for Computer Analysis. *Mol. Pharmacol. 47*, 1197−1203.

(11) Munson, P. J., and Rodbard, D. (1988) An Exact Correction to the "Cheng-Prusoff" Correction. *J. Recept. Res. 8*, 533−546.

(12) Case, D. A., Darden, T. A., Cheatham, T. E., III, Simmerling, C. L., Wang, J., Duke, R. E., Luo, R., Merz, K. M., Wang, B., Pearlman, D. A., Crowley, M., Brozell, S., Tsui, V., Gohlke, H., Mongan, J., Hornak, V., Cui, G., Beroza, P., Schafmeister, C., Caldwell, J. W., Ross, W. S., and Kollman, P. A. (2004), *AMBER 8*, University of California, San Francisco.

(13) Friesner, R. A., Murphy, R. B., Repasky, M. P., Frye, L. L., Greenwood, J. R., Halgren, T. A., Sanschagrin, P. C., and Mainz, D. T. (2006) Extra Precision Glide: Docking and Scoring Incorporating a Model of Hydrophobic Enclosure for Protein-Ligand Complexes. *J. Med. Chem. 49*, 6177−6196.

(14) Shivakumar, D., Williams, J., Wu, Y., Damm, W., Shelley, J., and Sherman, W. (2010) Prediction of Absolute Solvation Free Energies Using Molecular Dynamics Free Energy Perturbation and the OPLS Force Field. *J. Chem. Theor. Comput. 6*, 1509−1519.

(15) Witter, D. J., Harrington, P., Wilson, K., Chenard, M., Fleming, J. C., Haines, B., Kral, A. M., Secrist, J. P., and Miller, T. A. (2008) Optimization of Biaryl Selective HDAC1&2 Inhibitors (SHI-1: 2). *Bioorg. Med. Chem. Lett. 18*, 726−731.

(16) Bressi, J. C., Jennings, A. J., Skene, R., Wu, Y., Melkus, R., De Jong, R., O'Connell, S., Grimshaw, C. E., Navre, M., and Gangloff, A. R. (2010) Exploration of the HDAC2 Foot Pocket: Synthesis and SAR of Substituted N-(2-Aminophenyl)benzamides. *Bioorg. Med. Chem. Lett. 20*, 3142−3145.

(17) Copeland, R. A. (2005) Evaluation of Enzyme Inhibitors In *Drug Discovery*, pp 113−132, 141−155, Wiley-Interscience, NJ.

(18) Cheng, Y.-C., and Prusoff, W. H. (1973) Relationship between the Inhibition Constant (K1) and the Concentration of Inhibitor Which Causes 50% Inhibition (I50) of an Enzymatic Reaction. *Biochem. Pharmacol. 22*, 3099−3108.

(19) USPTO Application 20090156825, 2009.

(20) Chou, C. J., Herman, D., and Gottesfeld, J. M. (2008) Pimelic Diphenylamide 106 Is a Slow, Tight-Binding Inhibitor of Class I Histone Deacetylases. *J. Biol. Chem. 51*, 35402−35409.

(21) Schultz, B. E., Misialek, S., Wu, J., Tang, J., Conn, M. T., Tahilramani, R., and Wong, L. (2004) Kinetics and Comparative Reactivity of Human Class I and Class IIb Histone Deacetylases. *Biochemistry 43*, 11083−11091.

(22) Beckers, T., Burkhardt, C., Wieland, H., Gimmnich, P., Ciossek, T., Maier, T., and Sanders, K. (2007) Distinct Pharmacological Properties of Second Generation HDAC Inhibitors with the Benzamide or Hydroxamate Head Group. *Int. J. Cancer 121*, 1138−1148.

(23) Methot, J. L., Chakravarty, P. K., Chenard, M., Close, J., Cruz, J. C., Dahlberg, W. K., Fleming, J., Hamblett, C. L., Hamill, J. E., Harrington, P., Harsch, A., Heidebrecht, R., Hughes, B., Jung, J., Kenific, C. M., Kral, A. M., Meinke, P. T., Middleton, R. E., Ozerova, N., Sloman, D. L., Stanton, M. G., Szewczak, A. A., Tyagarajan, S., Witter, D. J., Secrist, J. P., and Miller, T. A. (2008) Exploration of the Internal Cavity of Histone Deacetylase (HDAC) with Selective HDAC1/HDAC2 Inhibitors (SHI-1:2). *Bioorg. Med. Chem. Lett. 18*, 973−978.

(24) Butler, L. M., Agus, D. B., Scher, H. I., Higgins, B., Rose, A., Cordon-Cardo, C., Thaler, H. T., Rifkind, R. A., Marks, P. A., and Richon, V. M. (2000) Suberoylanilide Hydroxamic Acid, an Inhibitor of Histone Deacetylase, Suppresses the Growth of Prostate Cancer Cells in Vitro and in Vivo. *Cancer Res. 60*, 5165−5170.

(25) Bressan, A., Bigioni, M., Bellarosa, D., Nardelli, F., Irrisuto, C., Maggi, C. A., and Binaschi, M. (2010) Induction of a Less Aggressive Phenotype in Human Colon Carcinoma HCT116 Cells by Chronic Exposure to HDAC Inhibitor SAHA. *Oncol. Rep. 24*, 1249−1255.